Hindawi Publishing Corporation
Advances in High Energy Physics
Volume 2008, Article ID 459290, 12 pages
doi:10.1155/2008/459290

Research Article

Black Hole Interior from Loop Quantum Gravity

Leonardo Modesto

Department of Physics, Bologna University, and INFN Bologna, Via Irnerio 46, 40126 Bologna, Italy

Correspondence should be addressed to Leonardo Modesto, lmodesto@perimeterinstitute.ca

Received 10 September 2008; Accepted 16 November 2008

Recommended by K. S. Viswanathan

We calculate modifications to the Schwarzschild solution by using a semiclassical analysis of loop quantum black hole. We obtain a metric inside the event horizon that coincides with the Schwarzschild solution near the horizon but that is substantially different at the Planck scale. In particular, we obtain a bounce of the S^2 sphere for a minimum value of the radius and that it is possible to have another event horizon close to the $r = 0$ point.

1. Introduction

Quantum gravity, the theory that wants to reconcile general relativity and quantum mechanics, is one of the major problems in theoretical physics today. General relativity tells that because also the space-time is dynamical, it is not possible to study other interactions on a fixed background. The background itself is a dynamical field.

Among the quantum gravity theories, a theory called "loop quantum gravity" [1–5] is the most widespread nowadays. This is one of the nonperturbative and background independent approaches to quantum gravity (another nonperturbative approach to quantum gravity is called "asymptotic safety quantum gravity" [6]). In the last years, the applications of loop quantum gravity ideas to minisuperspace models lead to some interesting results to solve the problem of space-like singularity in quantum gravity. As shown in cosmology [7–10], and recently, in black hole physics [11–16], it is possible to solve the cosmological singularity problem and the black hole singularity problem by using the tools and ideas developed in full loop quantum gravity theory. In the other well-known approach to quantum gravity, the called "asymptotic safety quantum gravity," authors [17, 18], using the G_N running coupling constant obtained in "asymptotic safety quantum gravity," have showed that nonperturbative quantum gravity effects give a much less singular Schwarzschild metric and that for particular values of the black hole mass it is possible to have the formation of another event horizon.

In this paper, we study the space time inside the event horizon at the semiclassical level using a constant polymeric parameter δ (see [19] for an analysis of the black hole interior using a nonconstant polymeric parameter). We consider the Hamiltonian constraint obtained in [15, 16]. In particular, we study the Hamiltonian constraint introduced in the first paper of reference [15, 16], where the authors have taken the general version of the constraint for real values of the Immirzi parameter γ.

This paper is organized as follows. In Section 2, we briefly recall the Schwarzschild solution inside the event horizon ($r < 2MG_N$) of [15, 16]. In Section 3, we introduce the Hamiltonian constraint in terms of holonomies and then the relative trigonometric form solving the Hamilton equations of motion. In Section 4, we give the metric form of the solution, and we discuss the new physics suggested by loop quantum gravity.

2. Schwarzschild solution inside the event horizon in Ashtekar variables

We recall the classical Schwarzschild solution inside the event horizon [15, 16]. For the homogeneous but nonisotropic Kantowski-Sachs space-time Ashtekar's, connection and density triads are (after the fixing of a residual global $SU(2)$ gauge symmetry on the spherically reduced phase space [15, 16])

$$\begin{aligned} A &= c\tau_3 dx + b\tau_2\, d\theta - b\tau_1 \sin\theta\, d\phi + \tau_3 \cos\theta\, d\phi, \\ E &= p_c \tau_3 \sin\theta \frac{\partial}{\partial x} + p_b \tau_2 \sin\theta \frac{\partial}{\partial \theta} - p_b \tau_1 \frac{\partial}{\partial \phi}. \end{aligned} \tag{2.1}$$

The components variables in the phase space can be read from the symmetric-reduced connection and density triad we can read the components variables in the phase space: (b, p_b), (c, p_c). The Poisson algebra is $\{c, p_c\} = 2\gamma G_N$, $\{b, p_b\} = \gamma G_N$. Following [15, 16], we recall that the classical Hamiltonian constraint in terms of the components variables is

$$\mathcal{C}_H = -\frac{1}{2\gamma G_N}\left[\left(b^2 + \gamma^2\right)\frac{p_b}{b} + 2cp_c\right] \tag{2.2}$$

in the gauge $N = \gamma \operatorname{sgn}(p_c)\sqrt{|p_c|}/16\pi G_N b$. Hamilton equations of motion are

$$\begin{aligned} \dot{b} = \{b, \mathcal{C}_H\} &= -\frac{b^2+\gamma^2}{2b}, \qquad \dot{p}_b = \{p_b, \mathcal{C}_H\} = \frac{1}{2}\left[p_b - \frac{\gamma^2 p_b}{b^2}\right], \\ \dot{c} = \{c, \mathcal{C}_H\} &= -2c, \qquad \dot{p}_c = \{p_c, \mathcal{C}_H\} = 2p_c. \end{aligned} \tag{2.3}$$

Solutions of (2.3) using the time parameter $t \equiv e^T$ and redefining the integration constant $\equiv e^{T_0} = m$ (see the first of papers in [15, 16]) are

$$\begin{aligned} b(t) &= \pm\gamma\sqrt{2m/t - 1}, \qquad p_b(t) = p_b^{(0)}\sqrt{t(2m-t)} \\ c(t) &= \mp\gamma m t^{-2}, \qquad p_c(t) = \pm t^2. \end{aligned} \tag{2.4}$$

This is exactly the Schwarzschild solution inside the event horizon as you can verify passing to the metric form defined by $h_{ab} = \mathrm{diag}(p_b^2/p_c, p_c, p_c \sin^2\theta)$ (m contains the gravitational constant parameter G_N).

3. Semiclassical dynamics from loop quantum gravity

We recall now the Hamiltonian constraint coming from "loop quantum black hole" [15, 16] in terms of the explicit trigonometric form of holonomies. The Hamiltonian constraint depends explicitly on the parameter δ that defines the length of the curves along which we integrate the connections to define the holonomies [15, 16]. We use the notation $\mathcal{C}^\delta$ for the hamiltonian constraint to stress the dependence on the parameter δ. The Hamiltonian constraint in terms of holonomies is

$$\begin{aligned}\mathcal{C}^\delta &= \frac{-N}{(8\pi G_N)^2\gamma^3\delta^3}\mathrm{Tr}\left[\sum_{ijk}\epsilon^{ijk}h_i^{(\delta)}h_j^{(\delta)}h_i^{(\delta)-1}h_j^{(\delta)-1}h_k^{(\delta)}\left\{h_k^{(\delta)-1},V\right\}+2\gamma^2\delta^2\tau_3 h_1^{(\delta)}\left\{h_1^{(\delta)-1},V\right\}\right]\\ &= -\frac{N}{2G_N\gamma^2}\left\{2\frac{\sin\delta c}{\delta}\frac{\sin\delta b}{\delta}\sqrt{|p_c|}+\left(\frac{\sin^2\delta b}{\delta^2}+\gamma^2\right)\frac{p_b\,\mathrm{sgn}(p_c)}{\sqrt{|p_c|}}\right\},\end{aligned} \tag{3.1}$$

where $V = 4\pi\sqrt{|p_c|}p_b$ is the spatial section volume, and we have calculated the Poisson brackets using the symplectic structure given in Section 2. The holonomies are

$$\begin{aligned}h_1^\delta &= \cos\frac{\delta c}{2}+2\tau_3\sin\frac{\delta c}{2},\\ h_2^\delta &= \cos\frac{\delta b}{2}-2\tau_1\sin\frac{\delta b}{2},\\ h_3^\delta &= \cos\frac{\delta b}{2}+2\tau_2\sin\frac{\delta b}{2}.\end{aligned} \tag{3.2}$$

Now, we can solve exactly the new Hamilton equations of motion if we take a gauge, where the equations for the canonical pairs (b, p_b) and (c, p_c) are decoupled. A useful gauge is $N = \gamma\sqrt{|p_c|}\mathrm{sgn}\,(p_c)\delta^2/\sin\delta b$ and in this particular gauge, the Hamiltonian constraint becomes

$$\mathcal{C}^\delta = -\frac{1}{2\gamma G_N}\left\{2\sin\delta c\, p_c+\left(\sin\delta b+\frac{\gamma^2\delta^2}{\sin\delta b}\right)p_b\right\}. \tag{3.3}$$

From (3.3), we obtain two independent sets of equations of motion on the phase space:

$$\begin{aligned}\dot{c} &= -2\sin\delta c, & \dot{p}_c &= 2\delta p_c\cos\delta c,\\ \dot{b} &= -\frac{1}{2}\left(\sin\delta b+\frac{\gamma^2\delta^2}{\sin\delta b}\right), & \dot{p}_b &= \frac{\delta}{2}\cos\delta b\left(1-\frac{\gamma^2\delta^2}{\sin^2\delta b}\right)p_b.\end{aligned} \tag{3.4}$$

Solving the first two equations for $c(T)$ and $p_c(T)$, we obtain

$$c(T) = \frac{2}{\delta}\arctan\left(\mp\frac{\gamma\delta m p_b^{(0)}}{2}e^{-2\delta T}\right),$$
$$p_c(T) = \pm e^{-2\delta T}\left[\left(\frac{\gamma\delta m p_b^{(0)}}{2}\right)^2 + e^{4\delta T}\right]. \tag{3.5}$$

Introducing a new time parameterization $t \equiv e^{\delta T}$, we obtain

$$c(t) = \frac{2}{\delta}\arctan\left(\mp\frac{\gamma\delta m p_b^{(0)}}{2t^2}\right) \longrightarrow \mp\frac{\gamma m p_b^{(0)}}{t^2},$$
$$p_c(t) = \pm\frac{1}{t^2}\left[\left(\frac{\gamma\delta m p_b^{(0)}}{2}\right)^2 + t^4\right] \longrightarrow \pm t^2. \tag{3.6}$$

In (3.6), we have calculated the small δ limit for the solutions $c(t)$ and $p_c(t)$, obtaining the Schwarzschild solution of paragraph one in (2.4) and calculated in [15, 16]. A substantial difference between the Schwarzschild solution and the solution (3.6) is that in the second case, there is an absolute minimum in $t_{\min} = (\gamma\delta m p_b^{(0)}/2)^{1/2}$, where p_c assumes the value $p_c(t_{\min}) = \gamma\delta m p_b^{(0)} > 0$. In Section 4, we will analyze the new physics coming from loop quantum gravity Hamiltonian constraint.

At this point, we integrate the equation of motion for $b(t)$, obtaining the following solution (we write the solution in the time coordinate t):

$$\cos\delta b = \sqrt{1+\gamma^2\delta^2}\left[\frac{\sqrt{1+\gamma^2\delta^2}+1-(2m/t)^{\sqrt{1+\gamma^2\delta^2}}\left(\sqrt{1+\gamma^2\delta^2}-1\right)}{\sqrt{1+\gamma^2\delta^2}+1+(2m/t)^{\sqrt{1+\gamma^2\delta^2}}\left(\sqrt{1+\gamma^2\delta^2}-1\right)}\right]. \tag{3.7}$$

To calculate $p_b(t)$, we introduce the solutions $c(t)$, $p_c(t)$, $b(t)$ in the Hamiltonian constraint, and we obtain $p_b(t)$ from the algebraic constraint equation $C^\delta = 0$. The solution of this equation gives $p_b(t)$ as function of the other phase space functions:

$$p_b(t) = -\frac{2\sin\delta c\sin\delta b\, p_c}{\sin^2\delta b + \gamma^2\delta^2}. \tag{3.8}$$

To obtain the explicit form of $p_b(t)$ in terms of the time coordinate t, it is sufficient to introduce in (3.8) the solution $\cos\delta b$ calculated in (3.7).

We note that the solution is homogeneous until it satisfied the trigonometric property $\cos\delta b \geq -1$. Using (3.7), we can calculate the variable t value (we define this t^*) until the solution is of Kantowski-Sachs-type, and we obtain

$$t^* = 2m\left(\frac{\sqrt{1+\gamma^2\delta^2}-1}{\sqrt{1+\gamma^2\delta^2}+1}\right)^{2/\sqrt{1+\gamma^2\delta^2}}. \tag{3.9}$$

However, we are interested in the semiclassical limit of the solution defined by $\delta \ll 1$, then in this particular limit $t^* \sim 0$ (see also Section 4).

Following [15, 16], we study the trajectory on the plane $p_c - p_b$, and we compare the result with the Schwarzschild solution of Section one. In Figure 1, we have a parametric plot of p_c and p_b (for $m = 10$) and $\gamma\delta \sim 1$ to amplify the quantum gravity effects in the plot (see Section 4). We can observe the substantial difference with the classical case. In the classical case (red line in Figure 1), $p_c \to 0$ for $t \to 0$, and this point corresponds to the classical singularity. In the semiclassical case instead, we start from $t = 2m$, where $p_c \to (2m)^2$ and $p_b \to 0$ (this point corresponds to the Schwarzschild horizon) and decreasing t, we arrive to a minimum value for $p_{c,m} \equiv p_c(t_{\min}) > 0$. From this point, p_c starts to grow another time until it assumes a maximum value for $p_b = 0$ that corresponds to a new horizon in $t = t^*$ localized (see Section 4, where we study the metric form of the solution). Our analysis refers to the region $t^* \leq t \leq 2m$, and the plot in Figure 1 refers to this time interval. The solution calculated is regular in the region $t^* \leq t \leq 2m$; in fact the cotriad ω [15, 16] defined by (it is the inverse of the triad E)

$$\omega = \frac{\operatorname{sgn}(p_c)|p_b|\tau_3}{\sqrt{|p_c|}}dx + \operatorname{sgn}(p_b)\sqrt{|p_c|}\tau_2 d\theta - \operatorname{sgn}(p_b)\sqrt{|p_c|}\tau_1 \sin\theta\, d\phi \tag{3.10}$$

is regular for all p_c in the region $t^* \leq t \leq 2m$.

4. Metric form of the solution

In this section, we present the metric form of the solution and we give a plot for any component of the Kantowski-Sachs metric $ds^2 = -N^2(t)dt^2 + X^2(t)dr^2 + Y^2(t)(d\theta^2 + \sin\theta\, d\phi^2)$. We start recalling the relation between connection and metric variables:

$$Y^2(t) = |p_c(t)|, \qquad X^2(t) = \frac{p_b^2(t)}{|p_c(t)|}, \qquad N^2(t) = \frac{\gamma^2\delta^2|p_c(t)|}{(16\pi G_N)^2 t^2 \sin^2\delta b}. \tag{4.1}$$

We give now the explicit form of the metric components in terms of the temporal coordinate t. The lapse function $N(t)$ is

$$(16\pi G_N)^2 N^2(t) = \frac{\gamma^2\delta^2\left[(\gamma\delta m/2t^2)^2+1\right]}{1-(1+\gamma^2\delta^2)\left[(M+1-Q)/(M+1+Q)\right]^2}, \tag{4.2}$$

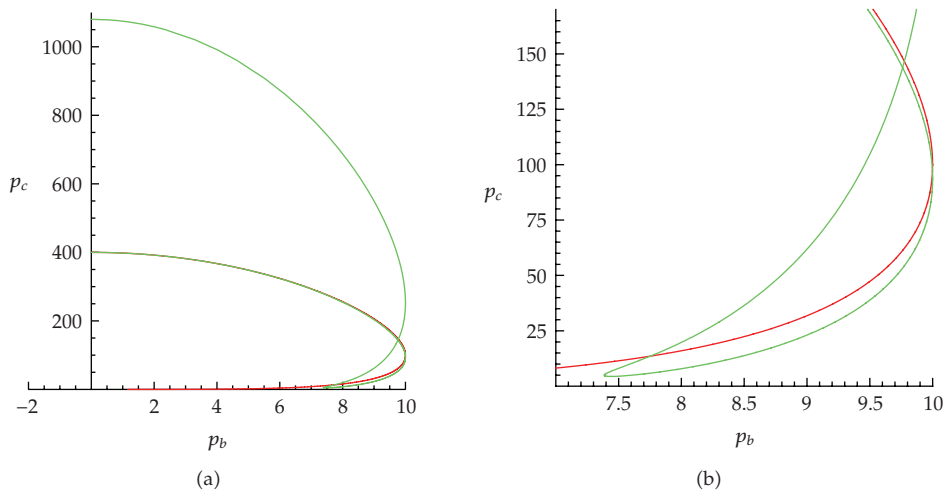

Figure 1: Semiclassical dynamical trajectory in the plane $p_b - p_c$. The plots for $p_c > 0$ and for $p_c < 0$ are disconnected and symmetric, but we plot only the positive values of p_c. The red trajectory corresponds to the classical Schwarzschild solution and the green trajectory corresponds to the semiclassical solution (the green and red curves are continuum curves). In the plot on the right, we have enlarged the region near the p_b axis.

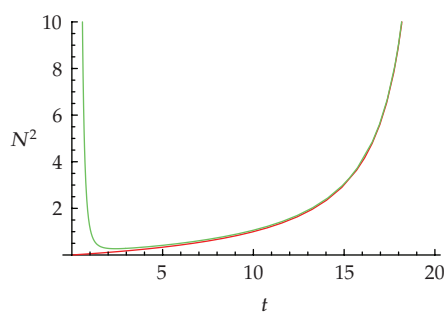

Figure 2: Plot of the lapse function $N^2(t)$ for $m = 10$ and $\gamma\delta \sim 1$ (in the horizontal axis, we have the temporal coordinate t and in the vertical axis, we have the lapse function). The red trajectory corresponds to the classical Schwarzschild solution inside the event horizon, and the green trajectory corresponds to the semiclassical solution.

where M denotes $\sqrt{1+\gamma^2\delta^2}$ and Q denotes $(2m/t)^{\sqrt{1+\gamma^2\delta^2}}(\sqrt{1+\gamma^2\delta^2}-1)$. In Figure 2, we have compared the classical Schwarzschild solution inside the event horizon with the solution (4.2) for $m = 10$ and $\gamma\delta \sim 1$ (we have taken $\gamma\delta \sim 1$ to amplify, in the plot, the loop quantum gravity modifications at the Planck scale). We can observe that the two solutions are identically when we approach to the event horizon (in which $t = 20$ in the units used in the plot) but are very different when we go toward $t \sim 0$. As we have explained in Section 3, we consider the region $t > t^*$ and for $t = t^*$ the lapse function diverges $N^2(t^*) \to +\infty$. The semiclassical solution has a minimum before diverging in $t = t^*$. In the classical solution instead (it is represented in red in Figure 2), $N^2(t)$ is very small for $t = t^*$ and it goes to zero for $t \to 0$.

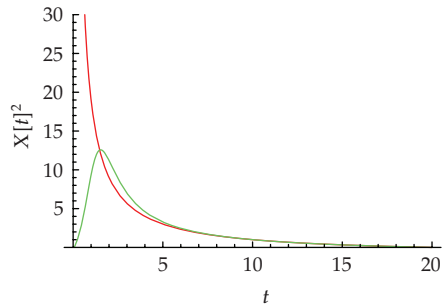

Figure 3: Plot of $X^2(t)$ for $m = 10$ and $\gamma\delta \sim 1$ (in the horizontal axis, we have the temporal coordinate t, and in the vertical axis we have $Y^2(t)$). The red trajectory corresponds to the classical Schwarzschild solution and the green trajectory corresponds to the semiclassical solution.

The anisotropy function $X^2(t)$ is related to $p_b(t)$ and $p_c(t)$ by (4.1), then by introducing (3.8) and (3.6) in the second relation of (4.1), we obtain

$$X^2(t) = \frac{(2\gamma\delta m)^2\left(1-\left(1+\gamma^2\delta^2\right)\left[(M+1-Q)/(M+1+Q)\right]^2\right)t^2}{(1+\gamma^2\delta^2)^2\left(1-\left[(M+1-Q)/(M+1+Q)\right]^2\right)^2\left[\left(\gamma\delta m p_b^{(0)}/2\right)^2+t^4\right]}, \tag{4.3}$$

where M denotes $\sqrt{1+\gamma^2\delta^2}$ and Q denotes$(2m/t)^{\sqrt{1+\gamma^2\delta^2}}(\sqrt{1+\gamma^2\delta^2}-1)$. Figure 3 represents a plot of $X^2(t)$, in this case too, the semiclassical solution reduces to the classical solution when t approaches the horizon but it is substantially different in the Planck region (we recall that in the plot, we have chosen $\gamma\delta \sim 1$ to amplify the quantum correction to Schwarzschild solution, but a semiclassical analysis is correct for $\delta \sim 10^{-33}$).

(In [15, 16], the spectrum of the operator $\widehat{p}_c$ was calculated as follows:

$$\widehat{p}_c|\mu,\tau\rangle = \gamma l_P^2 \tau|\mu,\tau\rangle. \tag{4.4}$$

In this paper, we have used dimensionless variables then the parameter δ, which is related to the area eigenvalues by (4.4), is of order $\delta \sim 10^{-33}$. The correct coefficient is $2\sqrt{3}$ and it is calculated in the first of [15, 16] comparing the area eigenvalues in the reduced Kantowski-Sachs model with the minimum area eigenvalue in full loop quantum gravity [20, 21].)

For the anisotropy as well as for the lapse function, it is important to remember that the solution refers to the region $t > t^*$, while for $t = t^*$, the anisotropy goes toward zero, $X(t^*) \to 0$. We can conclude that for $t = t^*$, we have another event horizon; in fact for this particular value of the time coordinate, the lapse function diverges and contemporary the anisotropy goes to zero. This result is qualitatively similar to the modified Schwarzschild solution obtained in asymptotic safe gravity [6] for particular values of the black hole mass [17, 18]. However, t^* is very small in our semiclassical analysis, and in this region, a complete quantum analysis of the problem is inevitable as developed in [15, 16].

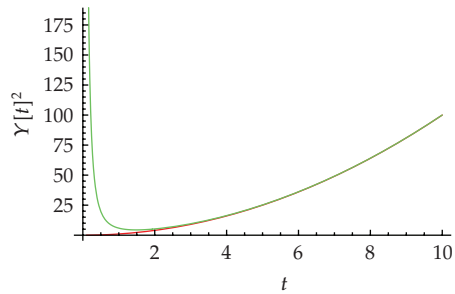

Figure 4: Plot of $\Upsilon^2(t)$ for $m = 10$ and $\gamma\delta \sim 1$ (in the horizontal axis, we have the temporal coordinate t; in the vertical axis, we have $\Upsilon^2(t)$). The red trajectory corresponds to the classical Schwarzschild solution, and the green trajectory corresponds to the semiclassical solution.

The metric component $\Upsilon^2(t)$ represents the square radius of the two-sphere S^2 and it is related to the density triad component $p_c(t)$ by the first relation reported in (4.1). Using the solution (3.6), we obtain

$$\Upsilon^2(t) = \frac{1}{t^2}\left[\left(\frac{\gamma\delta m p_b^{(0)}}{2}\right)^2 + t^4\right]. \tag{4.5}$$

In Figure 4, we have a plot of $\Upsilon^2(t)$ and we can note a substantial difference with the classical solution. In the classical case, the S^2 two-sphere goes to zero for $t \to 0$, in our semiclassical solution instead the S^2 sphere bounces on a minimum value of the radius, which is $\Upsilon^2(t_{\min}) = \gamma\delta m$, and it expands again to infinity for $t \to 0$. (We have taken the integration parameter $p_b^{(0)} = 1$ to match with the classical Schwarzschild solution near the horizon, see (2.4) and the first of [15, 16].) The minimum of $\Upsilon^2(t)$ corresponds to the time coordinate $t_{\min} = (m\gamma\delta/2)^{1/2}$ and $t^{\min} \gg t^*$, in fact $t^* \sim m\delta^4$ but $t_{\min} \sim (m\delta)^{1/2}$, then for $\delta \to 0$ (we have showed that $\delta \sim 10^{-33}$), we obtain $t_* \ll t_{\min}$.

In Figure 5, we have a plot of the spatial section volume $V \sim X(t)\Upsilon^2(t)$ and we can see that the semiclassical volume has a substantially different structure at the Planck scale, where it shows a maximum for $t > t^*$ and it goes to zero for $t = t^*$. The volume goes toward zero on the event horizons but this is not a problem for the singularity resolution because the horizons are coordinate singularities and not essential singularities.

Quantum ambiguities and semiclassical solution

In this paragraph, we want to compare the quantum spectrum of the operator $\widehat{1/|p_c|}$ with the semiclassical solution (4.5). At the quantum level, the spectrum of $\widehat{1/|p_c|}$, for a generic $SU(2)$ representation j is [22]

$$\widehat{\frac{1}{|p_{c,j}|}}|\mu,\tau\rangle = \left(\frac{3}{\gamma^{1/2}\delta\, l_P j(j+1)(2j+1)}\sum_{k=-j}^{k=j}\left[k\left(\sqrt{|\tau|} - \sqrt{|\tau - 2k\delta|}\right)\right]\right)^2 |\mu,\tau\rangle. \tag{4.6}$$

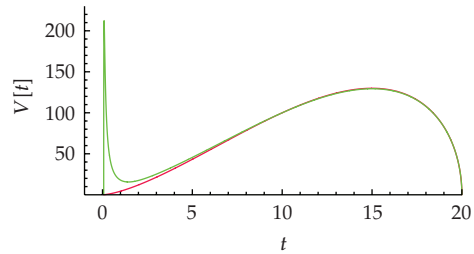

Figure 5: Plot of the spatial section volume $V \sim X(t)Y^2(t)$ for $m = 10$ and $\gamma\delta \sim 1$ (in the horizontal axis, we have the temporal coordinate t). The red trajectory corresponds to the classical volume, and the green trajectory corresponds to the semiclassical one. From the pictures, it is possible to note that the semiclassical volume (green line) is zero for $t = t^*$.

To compare the quantum spectrum with the semiclassical solution, we must have a relation between the eigenvalue τ and the temporal coordinate t. We calculate this relation comparing the large τ limit of (4.6) and the semiclassical solution near the horizon. The limit of (4.6) for large eigenvalues gives

$$\widehat{\frac{1}{|p_{c,j}|}}|\mu,\tau\rangle \longrightarrow_{\tau} \frac{1}{\gamma l_P^2|\tau|}|\mu,\tau\rangle, \tag{4.7}$$

and on the other side, we know that near the event horizon $1/|p_c| \to 1/t^2$, then comparing with (4.7), we obtain $\tau = t^2/\gamma l_P^2$. At this point, we have all the ingredients to compare the quantum operator spectrum with the semiclassical solution. From the plot in Figure 6, it is natural to interpret the semiclassical solution as the smooth approximation of the quantum operator spectrum but the similarity between semiclassical and quantum spectra is very stringent only if we choose a particular relation between the black hole mass and the $SU(2)$ representation j (in Figure 6, we have chosen $m = 400$ and $j = 100$). Using an heuristic argument, we can obtain the general relation between m and j. The relation is $m = 4j$ and now we go to show the validity of this mass quantization formula.

In Figure 7, we have represented with a green line the quantum spectrum and with a red line the semiclassical solution for some values of the representation j and of the mass m. This plot suggests the possibility to interpret the representation ambiguities in (4.6) as a label for the mass m (this idea remembers a recent result about the possibility to see ordinary matter as particular states in pure loop quantum gravity [23]). In fact in the semiclassical solution, we have a free parameter that corresponds to the black hole mass, and on the other side in the quantum spectrum, we have the representation j as a free parameter. If we interpret the semiclassical solution as the smooth approximation of the quantum spectrum, it is possible to match the time coordinate of the maximum for the two solutions. This is possible only if we choose a particular relation between m and the representation j. To obtain this relation, we calculate the derivative of the spectrum (4.6) with respect to τ and we evaluate the derivative in $\tau = t_{\min}^2/\gamma = m\delta/2$ (t is dimensionless in our analysis)

$$\partial_\tau\left(\frac{1}{\sqrt{p_{\tau,j}}}\right)\bigg|_{\tau=m\delta/2} = \frac{3}{2\delta\, j(j+1)(2j+1)}\sum_{k=-j}^{k=j}\left[k\left(\sqrt{\frac{2}{m}} - \sqrt{\frac{2}{m-4k}}\right)\right], \tag{4.8}$$

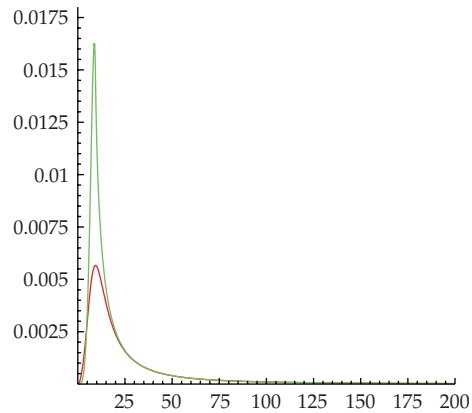

Figure 6: In this plot, we compare the semiclassical solution $1/Y^2(t)$ and the spectrum of the quantum operator $\widehat{1/|p_c|}$ for $j = 100$ and $m = 400$. The semiclassical solution is represented by a red line and the quantum spectrum by the green line one.

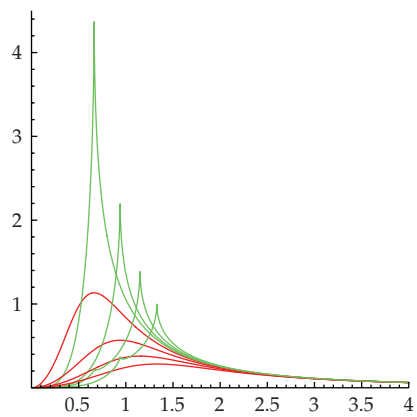

Figure 7: In this plot, we compare the semiclassical solution $1/Y^2(t)$ and the spectrum of the quantum operator $\widehat{1/|p_c|}$ to three particular values of the pair (j, m). From the left to the right in the plot, we consider four particular values of the pairs $(1/2, 2)$, $(1, 4)$, $(3/2, 6)$, $(2, 8)$, and $\gamma\delta \sim 1$. The semiclassical solution is represented by the red line and the quantum spectrum by the green one.

where p_τ is the eigenvalue of $\widehat{1/|p_c|}$. Observing (4.8), we see that in the $\widehat{1/|p_c|}$ spectrum the relative and absolute maximums correspond to points, where the derivative is divergent. Those points are in $m = 4j$ localized and this relation is also the mass quantization formula in Planck units. For any fixed value of the representation j, the classical black hole mass corresponds to the absolute maximum of the quantum spectrum in such representation.

5. Conclusions

In this paper, we have solved the Hamilton equation of motion for the Kantowski-Sachs space-time using the regularized Hamiltonian constraint suggested by loop quantum gravity. We have obtained a solution reproducing the Schwarzschild solution near the event horizon but that is substantially different in the Planck region near the point $r = 0$, where the

Table 1

$g_{\mu\nu}$	Semiclassical	Classical
$-N^2(t)$	$-\dfrac{\gamma^2\delta^2\left[\left(\dfrac{\gamma\delta m}{2t^2}\right)^2+1\right]}{1-(1+\gamma^2\delta^2)\left[\dfrac{\sqrt{1+\gamma^2\delta^2}+1-(2m/t)^{\sqrt{1+\gamma^2\delta^2}}\left(\sqrt{1+\gamma^2\delta^2}-1\right)}{\sqrt{1+\gamma^2\delta^2}+1+(2m/t)^{\sqrt{1+\gamma^2\delta^2}}\left(\sqrt{1+\gamma^2\delta^2}-1\right)}\right]^2}$	$-\dfrac{1}{(2m/t)-1}$
$X^2(t)$	$\dfrac{(2\gamma\delta m)^2\left(1-(1+\gamma^2\delta^2)\left[\dfrac{\sqrt{1+\gamma^2\delta^2}+1-(2m/t)^{\sqrt{1+\gamma^2\delta^2}}\left(\sqrt{1+\gamma^2\delta^2}-1\right)}{\sqrt{1+\gamma^2\delta^2}+1+(2m/t)^{\sqrt{1+\gamma^2\delta^2}}\left(\sqrt{1+\gamma^2\delta^2}-1\right)}\right]^2\right)t^2}{(1+\gamma^2\delta^2)^2\left(1-\left[\dfrac{\sqrt{1+\gamma^2\delta^2}+1-(2m/t)^{\sqrt{1+\gamma^2\delta^2}}\left(\sqrt{1+\gamma^2\delta^2}-1\right)}{\sqrt{1+\gamma^2\delta^2}+1+(2m/t)^{\sqrt{1+\gamma^2\delta^2}}\left(\sqrt{1+\gamma^2\delta^2}-1\right)}\right]^2\right)^2\left[\left(\dfrac{\gamma\delta m}{2}\right)^2+t^4\right]}$	$\dfrac{2m}{t}-1$
$Y^2(t)$	$\dfrac{1}{t^2}\left[\left(\dfrac{\gamma\delta m}{2}\right)^2+t^4\right]$	t^2

singularity is (classically) localized. The structure of the solution suggests the possibility to have another event horizon near the point $r = 0$ (this is similar to the result in "asymptotic safety quantum gravity" [17, 18], but the radius of such horizon is smaller than the Planck length and in this region a complete quantum analysis of the problem is inevitable [15, 16]).

Another interesting result is related to the S^2 sphere part of the three metrics. We obtain that in the semiclassical analysis, the radius of the two-sphere does not vanish, as in the classical case, but the sphere bounces on a minimum radius and it expands again to infinity. The solution is summarized in Table 1.

Using a heuristic argument, we have calculated the mass quantization formula comparing the semiclassical and quantum spectra of the inverse of the S^2 sphere square radius, $1/|p_c|$. Our arguments suggests that the mass spectrum formula $m = 4j$.

It is possible that the semiclassical analysis performed here will shed light on the problem of the "information loss" in the process of black hole formation and evaporation. See, in particular [24] for a possible physical interpretation of the black hole information loss problem.

Acknowledgment

The author is grateful to Roberto Balbinot, Alfio Bonanno, and Eugenio Bianchi for many important and clarifying discussions.

References

[1] C. Rovelli, *Quantum Gravity*, Cambridge University Press, Cambridge, UK, 2004.
[2] A. Ashtekar and J. Lewandowski, "Background independent quantum gravity: a status report," *Classical and Quantum Gravity*, vol. 21, no. 15, pp. R53–R152, 2004.
[3] T. Thiemann, "Loop quantum gravity: an inside view," in *Approaches to Fundamental Physics*, vol. 721 of *Lecture Notes in Physics*, pp. 185–263, Springer, Berlin, Germany, 2007.

[4] T. Thiemann, "Introduction to modern canonical quantum general relativity," submitted, http://arxiv.org/abs/gr-qc/0110034.
[5] T. Thiemann, "Lectures on loop quantum gravity," in *Quantum Gravity*, vol. 631 of *Lecture Notes in Physics*, pp. 41–135, Springer, Berlin, Germany, 2003.
[6] M. Reuter, "Nonperturbative evolution equation for quantum gravity," *Physical Review D*, vol. 57, no. 2, pp. 971–985, 1998.
[7] M. Bojowald, "Inverse scale factor in isotropic quantum geometry," *Physical Review D*, vol. 64, no. 8, Article ID 084018, 8 pages, 2001.
[8] M. Bojowald, "Loop quantum cosmology: IV. Discrete time evolution," *Classical and Quantum Gravity*, vol. 18, no. 6, pp. 1071–1087, 2001.
[9] M. Bojowald, "Loop quantum cosmology: recent progress," *Pramana*, vol. 63, no. 4, pp. 765–776, 2004.
[10] A. Ashtekar, M. Bojowald, and J. Lewandowski, "Mathematical structure of loop quantum cosmology," *Advances in Theoretical and Mathematical Physics*, vol. 7, no. 2, pp. 233–268, 2003.
[11] L. Modesto, "Disappearance of the black hole singularity in loop quantum gravity," *Physical Review D*, vol. 70, no. 12, Article ID 124009, 5 pages, 2004.
[12] L. Modesto, "The Kantowski-Sachs space-time in loop quantum gravity," *International Journal of Theoretical Physics*, vol. 45, no. 12, pp. 2235–2246, 2006.
[13] L. Modesto, "Gravitational collapse in loop quantum gravity," *International Journal of Theoretical Physics*, vol. 47, no. 2, pp. 357–373, 2008.
[14] L. Modesto, "Quantum gravitational collapse," submitted, http://arxiv.org/abs/gr-qc/0504043.
[15] A. Ashtekar and M. Bojowald, "Quantum geometry and the Schwarzschild singularity," *Classical and Quantum Gravity*, vol. 23, no. 2, pp. 391–411, 2006.
[16] L. Modesto, "Loop quantum black hole," *Classical and Quantum Gravity*, vol. 23, no. 18, pp. 5587–5601, 2006.
[17] A. Bonanno and M. Reuter, "Renormalization group improved black hole spacetimes," *Physical Review D*, vol. 62, no. 4, Article ID 043008, 21 pages, 2000.
[18] A. Bonanno and M. Reuter, "Spacetime structure of an evaporating black hole in quantum gravity," *Physical Review D*, vol. 73, no. 8, Article ID 083005, 10 pages, 2006.
[19] C. G. Böhmer and K. Vandersloot, "Loop quantum dynamics of the Schwarzschild interior," *Physical Review D*, vol. 76, no. 10, Article ID 104030, 11 pages, 2007.
[20] C. Rovelli and L. Smolin, "Loop space representation of quantum general relativity," *Nuclear Physics B*, vol. 331, no. 1, pp. 80–152, 1990.
[21] C. Rovelli and L. Smolin, "Discreteness of area and volume in quantum gravity," *Nuclear Physics B*, vol. 442, no. 3, pp. 593–619, 1995.
[22] M. Bojowald, "Quantization ambiguities in isotropic quantum geometry," *Classical and Quantum Gravity*, vol. 19, no. 20, pp. 5113–5129, 2002.
[23] S. O. Bilson-Thompson, F. Markopoulou, and L. Smolin, "Quantum gravity and the standard model," *Classical and Quantum Gravity*, vol. 24, no. 16, pp. 3975–3993, 2007.
[24] A. Ashtekar and M. Bojowald, "Black hole evaporation: a paradigm," *Classical and Quantum Gravity*, vol. 22, no. 16, pp. 3349–3362, 2005.